Mass Transfer in Supported Froths

WALTER L. WORKMAN and SEYMOUR CALVERT

Case Institute of Technology, Cleveland, Ohio

Operating and mass transfer characteristics are reported for a supported froth apparatus consisting of a dual-flow sieve plate column with eggcrate packing above the plate. The assembled packing produced a series of vertical tubes and served to support the froth generated at the plate, increasing its height and consequently the contact time. Addition of the packing improved the mass transfer efficiency. Systems studied were ammonia–air–water and carbon dioxide–air–water. Effects of liquid and gas rate as well as packing size and spacing are correlated. A model based on measurable physical parameters was developed to predict efficiency, and a generalized correlation of efficiency was developed.

Froth equipment has come into widespread use as an effective contacting medium. Its growing popularity can be attributed to one or more of its basic characteristics: It usually offers less pressure drop than comparable bubbling equipment, and it offers more interfacial area per unit volume of liquid and is usually more efficient than other comparable equipment.

The present study grew out of the observations made in previous work with laboratory gas absorbers. These studies indicated that the effect of column diameter was important in determining froth height if the column diameter was small. A significant effect of column diameter was observed for columns less than 25 mm. in diameter (*4*). It was decided to investigate the possibility of providing a structure which would serve to support the froth and thereby increase its height.

One of the objectives of the design of the experimental apparatus was to provide a structure and a mode of operation such that the important physical parameters could be controlled and observed or measured. The basic apparatus chosen for study was a dual-flow sieve plate column. Support of the froth was increased by the addition of a special eggcrate packing above the plate. This packing consisted of Lucite sheets machined in a manner that would produce a series of vertical tubes when assembled. Photographs of the experimental column with the sieve place and eggcrate packing in place, and also of supported froth equipment in operation, can be found in reference 39.

A second part of the present study was to establish a mathematical model based upon measurable physical parameters which would be capable of accounting for important parameters in mass transfer and which would predict the efficiency of the froth equipment.

BACKGROUND AND THEORETICAL CONSIDERATIONS

The first phase of the present mass transfer work was the formulation of a model which incorporated the important variables of the system. This model was then used in conjunction with the variables reported and correlated in this paper to predict the mass transfer efficiency. Experimental determination of efficiency provided a means of checking the prediction.

For the present model it has been assumed that the outside mass transfer coefficient of the bubbles (the liquid phase coefficient) can be described in terms of the Higbie penetration theory (*16*). According to this theory, the transfer rate from the interface into the liquid is given by

$$k_L = \sqrt{\frac{4D_L}{t_r\,\pi}} \tag{1}$$

If t_r, the surface renewal time, is taken as the time required for the bubble to move through its diameter relative to the liquid, then

$$k_L = \sqrt{\frac{2D_L\,U_B}{\pi\,a}} \tag{2}$$

Where the diffusional process involves unsteady transfer to a stagnant sphere with an external resistance to transfer just outside the surface, Crank (*6*) shows that the process may be described by the following differential equation:

$$\frac{\partial C}{\partial r}\,D_g = \alpha(C_s - C_o) \tag{3}$$

α represents a surface condition that takes into account the external resistance to transfer. By equating the rates of transfer in the gas and liquid phase, by assuming that the solutions are dilute so Henry's law is obeyed, and also by assuming that the gases are ideal

$$\alpha = \frac{RT}{H}\,k_L \tag{4}$$

Crank (*6*) also shows that the solution for Equation (3) is

$$f_s = \frac{M_t}{M_\infty} = 1 - \sum_{n=1}^{\infty} \frac{6\,\Gamma\,2_e - B^2{}_n\left(\dfrac{D_g\,t_g}{a^2}\right)^{1/2}}{B^2{}_n\,[B^2{}_n + \Gamma\,(\Gamma - 1)]} \tag{5}$$

where

$$B_n\text{'s are the roots of:}\quad B_n \cot B_n + \Gamma - 1 = 0 \tag{6}$$

and

$$\Gamma = \frac{a\alpha}{D_g} \tag{7}$$

f_s is the intrinsic efficiency, defined as the ratio of the amount transferred at time t to the amount transferred at infinite time (equilibrium). A further significance of the parameter Γ can be seen by combining Equations (4) and (7):

$$\Gamma = \frac{a\,RT\,k_L}{D_g\,H} \tag{8}$$

Γ is a measure of the ratio of the resistances to transfer in the liquid and gas phases. If Γ is large the resistances will be primarily in the gas phase and the system will be gas phase controlled; if Γ is small the resistance will be mainly in the liquid phase and the system will be liquid phase controlled.

Walter L. Workman is with Union Carbide Corporation, South Charleston, West Virginia. Seymour Calvert is with Pennsylvania State University, University Park, Pennsylvania.

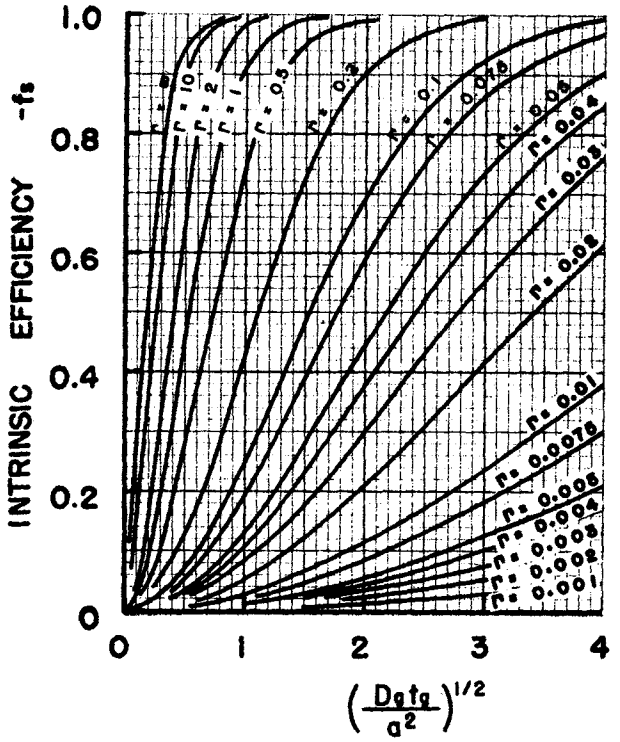

Fig. 1. Intrinsic efficiency vs. $(D_g t_g/a^2)^{1/2}$ with Γ as parameter.

The first ten roots of Equation (6) and the complete numerical solution of Equation (5) with Γ as a parameter are included in reference 39. Figure 1 is a graphical solution. These solutions were accomplished by programming the appropriate equations on the Burroughs 220 digital computer.

It has been assumed that the transfer inside the gas bubbles takes place by molecular diffusion. This assumption introduces no serious error into the solution for the case of true liquid phase controlling transfer. In the case of gas phase controlled systems the assumption sets the lower limit on the rate of transfer. Circulation and eddy diffusion inside the bubble would increase the rate. The consequence of an error made because of this assumption would be to predict a conservative estimate of the efficiency.

It has been assumed that the bubbles are spherical for the basic model. Where flow patterns or geometrical considerations affected the shape of the bubbles it became necessary to modify this assumption. An example is given in connection with predicting mass transfer results.

Efficiency

The efficiency used in this work will be termed *intrinsic efficiency*. It represents the fractional approach to equilibrium for a gas bubble and the liquid it contacts. Consider Figure 2. This case represents perfect mixing of the liquid, where all concentration gradients in the bulk liquid have been eliminated. The intrinisc efficiency is given by

$$f_s = \frac{P_i - P_f}{P_i - P^*} \qquad (9)$$

Consider Figure 3, however. Here the liquid phase in contact with gas is not perfectly mixed. Two examples of when this might happen are cocurrent flow and liquid recycle. A schematic representation of gas and liquid streams is shown at the right. The intrinsic efficiency is

$$f_c = \frac{P_i - P_f}{P_i - P_\infty} \qquad (10)$$

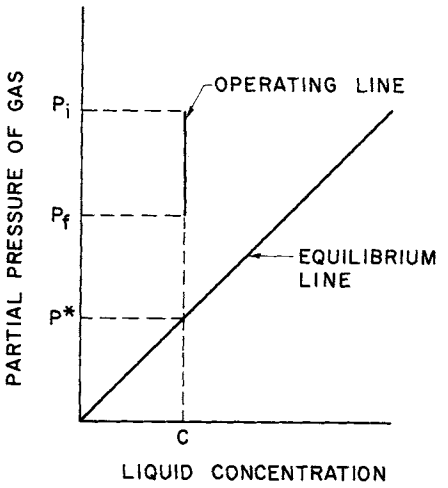

Fig. 2. Operating and equilibrium diagram. Perfect liquid mixing.

In every case it is noted that the intrinsic efficiency represents the ratio of the fraction of the gas phase removed to the fraction that could have been removed if the leaving gas stream had reached equilibrium with the liquid it contacted.

In mass transfer operations it is usually assumed that a line connecting the inlet and outlet concentrations on the operating diagram will represent the overall material balance line and that this line also represents the operating line for that stage. It is interesting to note that in the present study these assumptions are not valid.

Consider Figure 4. The inlet and outlet compositions of the entire stage are noted and a dotted line connects these points. Without additional information this would be taken as the operating line. A schematic diagram of the gas and liquid streams and corresponding concentrations is shown at the right. When fresh liquid with concentration C_1 was added to the stage, it was immediately mixed with liquid existing at the top of the stage. The resulting concentration was C_i. At random, one of the vertical tubes stopped its upward flow of gas and liquid and the liquid drained down through this tube to the top of the plate. The liquid did not contact the gas phase until it reached the bottom of the packed section. Gas and liquid were then carried cocurrently up the vertical tubes. The maximum concentration of dissolved gas in the liquid phase existed at the top of the tubes. As the liquid left the tubes it was mixed with the incoming liquid and returned to the bottom at concentration C_i. Because there was considerable mixing of the liquid phase there was no intermediate concentration corresponding to a point on the dotted line. The operating line, the

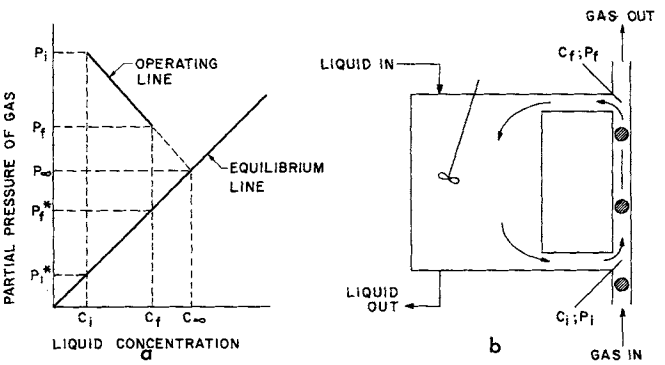

Fig. 3. (a) Operating and equilibrium diagram. (b) Schematic representation of gas and liquid streams with liquid recycle.

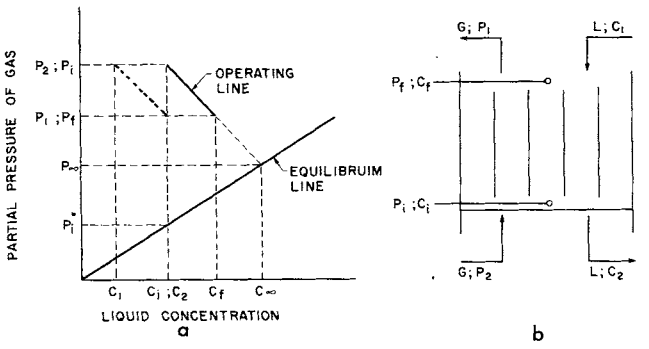

Fig. 4. (a) Operating and equilibrium diagram. (b) Schematic representation of gas and liquid streams supported froth equipment.

slope of which represented the effective gas-to-liquid ratio, was defined from the flow rates and compositions in the vertical tubes. The operating line is shown as the solid line in Figure 4 with its corresponding compositions noted.

The equilibrium compositions P_∞ and C_∞ were determined by the intersection of the operating and equilibrium lines. Because the fractional efficiency was low in the case of carbon dioxide, the change in gas concentration and the resulting slope of the operating line and its intersection with the equilibrium line could not be graphically determined with sufficient accuracy. It was, therefore, computed analytically.

As the gas and liquid travel up the tubes the liquid tends to become saturated with the transferring component. This affects the amount of solute which may be adsorbed and also reduces the driving force for mass transfer. Referring to Figure 4, the maximum driving force is $(P_i - P^*_i)$. This maximum driving force is realized only at the bottom of the column. The driving force at any position in the column is $(P_g - P^*_g)$, and varies continuously up the column. It is important therefore to account properly for this change in driving force caused by cocurrent flow of liquid and gas when computing the efficiency.

By referring again to Figure 4 and defining

$$m = \frac{P_i - P^*_i}{P_i - P_\infty} \tag{11}$$

then by geometry

$$m = 1 + \frac{GH}{LRT} \tag{11a}$$

If it is assumed that the transfer coefficients, total contact area, and contact time are equal for the perfectly mixed and cocurrent cases, the relationship between f_c and f_s [defined by Equations (9) and (10)] becomes

$$1 - f_c = (1 - f_s)^m \tag{12}$$

Predicted values of f_s were converted to the corresponding values of f_c by Equation (12).

For low efficiencies the change in gas concentration $(P_i - P_f)$ was small and extremely difficult to measure experimentally. It was also impossible to sample properly and determine the liquid concentration C_f. Consequently a method was established from which the efficiency f_c could be determined from the experimentally measurable quantities. For the gas stream the necessary quantity was the inlet concentration (P_2). For the liquid phase this was the inlet concentration (C_i). Once these quantities had been established the equilibrium gas composition (P^*) could be determined from the operating diagram. The gas composition (P_f) was computed from the overall material balance relationship.

The procedure followed was to compute the efficiency as if the liquid were perfectly mixed and then to correct for the effect of cocurrent flow.

For equal changes in gas concentration the relationship between f_s and f_c is

$$f_c = mf_s \tag{13}$$

The experimentally determined values of f_s were converted to values of f_c by Equation (13).

EXPERIMENTAL

Experimental Apparatus

The basic unit in the experimental apparatus was a dual-flow sieve plate column. The column was 4-in. × 4-in. square by 36-in. long. It consisted of aluminum framework and sides. The front and back were made of glass. The plate was located 12 in. above the bottom of the column. The sieve plate itself was made from 0.035-in. aluminum sheet. One-eighth-in. sharp edged holes were drilled on ¼-in. staggered centers. The plate contained 18.5% free area. Provisions were made for gas entry and water exit below the sieve plate, with water entry and gas vent above the plate. Gas and liquid sampling ports and pressure taps were provided above and immediately below the plate. A liquid leg was attached to the column at the level of the tray.

Packing, made from ⅛-in. Lucite sheet, was placed above the plate. It was machined in a manner which would make vertical square tubes when assembled. The packing sections were 4 in. in length. Three sizes of packing (tube diameter) were studied: ⅜, ⅝, and ⅞ in. This packing was separated from the tray by Lucite strips machined to various widths, the width depending upon the separation desired. When more than one section of packing was run this same procedure was used to separate the sections.

The entire experimental setup is shown in Figure 5. Details for the experimental apparatus may be found in reference 39.

Mass Transfer Systems Studied

The systems chosen for study were carbon dioxide–air–water and ammonia–air–water. The first is an example of a sparingly soluble gas and is a liquid phase controlled system. The second is considered to be predominantly gas phase controlling, although there is a slight dependence upon the liquid phase resistance. This may be caused by a limiting reaction in the liquid phase near the gas-liquid interface. A detailed discussion of available data and the magnitude to the correction is given by Sherwood and Pigford (29).

Photographic Techniques

It was necessary to determine bubble sizes and the velocity of the phases by a photographic technique. Details may be found in reference 39.

Still pictures made with a 35-mm. Miranda camera furnished most of the data for bubble sizes. A 3¼-in. × 4¼-in. Speed Graphic camera and a 16-mm. Bolex movie camera also were used to a limited extent for this purpose. The bubble sizes were also measured from prints in the case of the

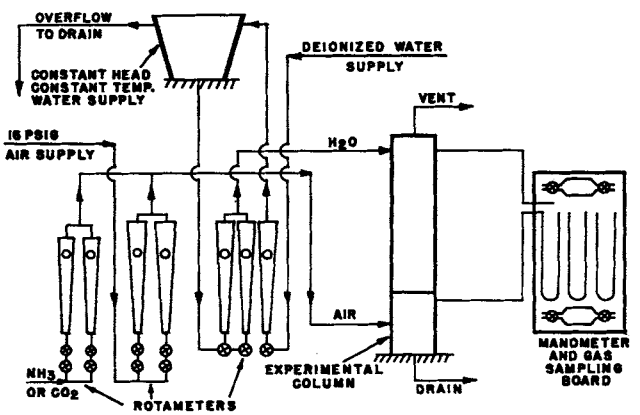

Fig. 5. Experiment setup.

Speed-Graphic camera. The movie film was viewed in a microfilm reader.

For determination of the velocity of the gas and liquid phases it was necessary to take high-speed movies, and a 16-mm. Fastax camera was used. It was operated at 840 and 1,236 frames/sec. The processed film was projected at 16 frames/sec. onto a screen which had been ruled with grid lines. A timer with divisions of 1/1,000 of a sec. was photographed alongside the column and was used to time the action in the projected pictures.

Analytical Techniques

Gas and liquid samples were analyzed by various methods. Details of the sampling procedures and the methods of analyses are in reference 39. In general, the techniques were as follows. Liquid samples containing carbon dioxide were analyzed by electrical conductivity and the results checked from time to time by titration. The titration procedure was to absorb the sample in excess barium hydroxide and back titrate the excess in the presence of barium chloride to a phenolphthalein end point. Gas samples containing carbon dioxide were generally analyzed by the gas chromatograph and the results checked by the same titration procedure as for the liquid samples. Liquid and gas samples containing ammonia were dissolved in excess hydrogen chloride and the excess acid back titrated with sodium hydroxide using a mixed indicator methyl red methylene blue. Early titrations were done with a pH meter in the presence of the indicator and the color change at the equivalence point noted. It was determined that the indicator alone gave sufficient accuracy and the tedious analysis with the pH meter was unnecessary.

RESULTS

Operating Limits and Flooding Characteristics

Addition of the packing in this study resulted in operating regions and flooding points not entirely comparable with those in other equipment. In the more common mass transfer equipment such as packed column, bubble cap trays, and cross-flow sieve trays, the pressure drop increases rapidly with increasing gas or liquid rate above a point referred to as the loading point. This loading point is followed at higher rates of gas and liquid by approach to an inoperable condition known as flooding. The point of the characteristic sharp break in the pressure drop curve at the loading point can be correlated as well as the flooding point (*20, 30*).

In the column studied there was no break in the pressure drop curve corresponding to that observed with most other equipment. Flooding of the column under normal operating regions of gas and liquid rates took the form of excessive entrainment. A critical, sharply defined point would be reached upon increasing gas rate where the water added to the packed section would tend to be suspended there and would not flow downward through the packing. This point was also accompanied by excessive entrainment of liquid. This was termed the *flooding point* and could be successfully determined by inspection.

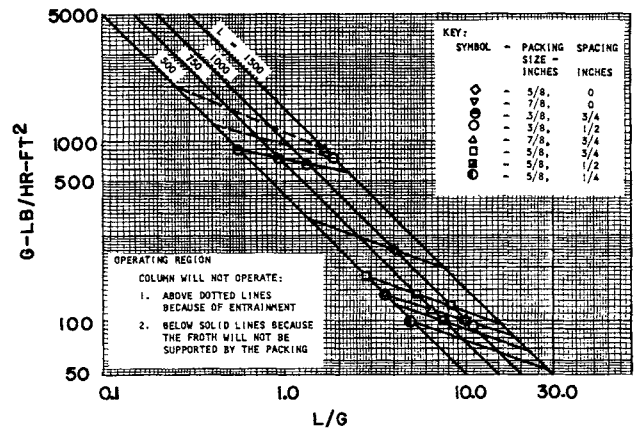

Fig. 6. Operating region, G vs. L/G.

At low values of G another boundary of the operating region could be defined. Below a certain value of G at a given L/G ratio the column would not operate. That is, the froth that was generated on the tray would not be supported by the packing. The froth broke up at the entrance to the vertical sections. The values of liquid and gas rates which defined this boundary are determined by the size of the packing and its spacing above the tray.

The operating region, or the region between the minimum value of G for operation of the packing and the point of flooding characterized by excessive entrainment, can be conveniently defined. Figure 6 shows this relationship; G is plotted as abscissa with L/G as ordinate. Parameters are packing size, packing spacing, and liquid rate. Details are shown in the figure. The results are similar to the flooding characteristics of unpacked vertical tubes (*25*).

The range of liquid and gas rates for which the column could be successfully operated was quite large. This depended upon the particular packing and spacing used. The magnitude of gas rates that could be run was about 100 to 2,000 lb./(hr.) (sq. ft.). This is about the same as that for conventional perforated plate column (*21*). For some combinations of packings and spacings, however, the gas rate could be varied about twentyfold. The average was about tenfold. This was a greater variation than that observed by Mayfield et al. (*21*) for conventional perforated plate column.

The range of liquid rates varied from 500 to 1,500 lb./(hr.) (sq. ft.) This was rather low for the liquid handling capacity of commercial equipment.

Froth Height

Effect of Liquid and Gas Rates. A series of experiments was performed to determine the effect of gas and liquid rates upon froth height. In these experiments the spacing between the tray and the packing was ½ in. When more than one section of packing was run the separation between the sections was also maintained at ½ in. In general it was found that froth height increased with both liquid and gas rates.

Because of the large amount of data accumulated and because of the cumbersome nature of working with the raw data, it was desirable to represent the results by an analytical expression. This expression was determined to be

$$h_2 = a_1 L^Q G^W \qquad (14)$$

The data accumulated from runs specifically designed for froth height studies as well as those from mass transfer runs were fitted to Equation (14) by a multiple regression analysis, performed by the Burroughs 220 digital computer with the MURA (*23*) program available on the computer. Table 1-*A* gives the constants a_1, Q, and W in Equation (14) for the ranges of L and G studied.

It is noted that the froth height is greater in the case of the ammonia-air-water system. It is felt this was caused by the lower surface tension of this system.

Effect of Spacing. A series of experiments was designed to determine the effect of packing spacing on froth height. In these experiments the liquid rate was maintained at a constant 1,000 lb./(hr.) (sq. ft.). Both one and two sections of packing were run; ⅜-, ⅝-, and ⅞-in. packings were studied and separations of 0-, ¼-, ½-, and ¾-in. were studied.

In general it was found that at small separations the froth height was low. It increased with increasing separation to a maximum value and fell beyond that point as the separation was increased further. If the increase in

spacing resulted in a region outside the operating region as defined by Figure 6, the column would no longer operate.

An analytical expression for representing the data is

$$h_2 = a_3 C_1^S G^W \qquad (15)$$

Table 1-*B* summarizes the results.

Effect of Packing Size. The heart of the first phase of this work centered around the idea of increasing the froth height by the addition of packing. Under every operating condition, except one, addition of packing achieved this goal. The only exception was the case of operating under conditions of excessive spacing. The relationships for froth height as a function of the operating variables have been given in the previous sections. As expected, the froth height was a maximum for the smallest packing and a minimum for the largest.

Liquid Holdup

It was necessary to determine liquid holdup for the computation of froth density and pressure drop. Liquid holdup was determined for the same conditions as the froth height. A peculiarity of the design of the sieve plate made direct measurement of the clear liquid height on the tray possible. Careful stoppage of the air supply would leave the liquid trapped above the plate. The height was then measured. The liquid holdup was computed from knowledge of clear liquid height and area of the column. The volume occupied by the packing material was subtracted from the total volume when computing the liquid holdup.

The expression for h_1 as a function of gas and liquid rates was found to be

$$h_1 = a_4 L^Q G^W \qquad (16)$$

Table 1-*C* is a tabulation of these constants.

TABLE 1.

A. Effect of liquid and gas rate on froth height
Tabulation of a_1, Q, and W in: $h_2 = a_1 L^Q G^W$

Packing designation*	System	a_1	Q	W	Maximum deviation of h_2, %
1-4, ⅜ (½)	Carbon dioxide	0.1398	0.3418	0.2472	7.9
1-4, ⅜ (½)	Ammonia	0.1062	0.3368	0.3242	—11.3
1-4, ⅝ (½)	Carbon dioxide	0.0326	0.4293	0.3803	7.8
1-4, ⅝ (½)	Ammonia	0.0996	0.2840	0.3590	—8.3
No packing	Ammonia	0.3592	0.1851	0.1813	0.5
No packing†	Carbon dioxide	0.3820	†	0.3282	

B. Effect of spacing on froth height
Tabulation of a_3, C_1, and W in: $h_2 = a_3 C_1^S G^W$

Packing designation*	System	a_3	C_1	W	Maximum deviation of h_2, %
1-4, ⅜	Carbon dioxide	1.909	2.033	0.1528	—7.8
1-4, ⅝	Carbon dioxide	2.139	2.365	0.1217	5.4
2-4, ⅝	Carbon dioxide	0.9336	0.9535	0.3247	—15.9
1-4, ⅞	Carbon dioxide	1.346	2.489	0.1964	3.8
2-4, ⅞	Carbon dioxide	0.9635	1.811	0.2716	—7.4

C. Effect of liquid and gas rate on clear liquid height
Tabulation of a_4, Q, and W in: $h_1 = a_4 L^Q G^W$

Packing designation*	System	a_4	Q	W	Maximum deviation of h_1, %
1-4, ⅜ (½)	Ammonia	0.0383	0.4300	0.1991	—13.4
1-4, ⅜ (½)	Carbon dioxide	0.5511	0.1551	0.0373	—10.6
1-4, ⅝ (¾)	Ammonia	0.0043	0.6348	0.2903	—16.5
1-4, ⅝ (¾)	Carbon dioxide	0.0337	0.3762	0.2406	11.5

D. Effect of spacing on clear liquid height
Tabulation of a_5, C_2, and W in: $h_1 = a_5 C_2^S G^W$

Packing designation*	System	a_5	C_2	W	Maximum deviation of h_1, %
1-4, ⅜	Carbon dioxide	1.164	2.121	0.0328	11.9
2-4, ⅜	Carbon dioxide	0.4293	3.756	0.2200	—11.8
1-4, ⅝	Carbon dioxide	1.523	2.009	0.0066	—12.4
2-4, ⅝	Carbon dioxide	1.327	1.082	0.1070	12.7
1-4, ⅞	Carbon dioxide	1.320	2.707	0.0375	—6.2

* Packing designation: No. of sections, height of section, size of tubes. All sizes are in inches. (Spacing of sections above tray and between sections when column is operated with more than one section.)
† For $L = 1{,}000$; $h_2 = a_1 G^W$.

The relationship for h_1 as a function of packing spacing was similar to that for h_2:

$$h_1 = a_5 C_2^S G^W \quad (17)$$

for all runs within the operating region. Table 1-D tabulates the results.

As in the case of froth height, h_1 was greater with the ammonia system.

Froth Density

A very important consideration is the froth density, defined as $\rho_f = h_1/h_2$. It is important in pressure drop predictions, which follow, and in determining the relationship between the superficial gas velocity and the velocity of a gas bubble. The froth density remained essentially constant for both systems studied.

Pressure Drop

In formulating an expression for pressure drop it was considered to be a result of three things. The perforated plate was considered to be a series of orifices. Above the plate a portion of the pressure drop was due to a hydrostatic head of liquid. The third consideration was the effect of friction as the two-phase mixture passed up through the vertical tubes.

The equation used to estimate the pressure drop caused by the orifice effect was

$$G'' = 0.68\sqrt{\frac{29}{MW} \times \frac{520}{T} \times Z \times P \sqrt{h}} \quad (18)$$

The contribution from hydrostatic head was considered to be clear head of liquid above the tray h_1.

The frictional loss was estimated from two-phase flow data and the two-phase pressure drop correlations of Govier et al. (*13, 14*). Basically the procedure consisted of using published values for a two-phase friction factor for vertical flow of air and water with the air and water velocities and liquid holdup ratios determined in the present work. The equations used were

$$h_f = \frac{1}{1 + R_v}\left(\frac{\Delta F}{\Delta X}\right) \quad (19)$$

where

$$\frac{\Delta F}{\Delta X} = \frac{2f'_L U^2_L}{g_c D'} \quad (20)$$

Here f'_L is the two-phase friction factor. Govier et al. (*13, 14*) have correlated f'_L with tube diameter and velocities of the gas and liquid phases.

The frictional loss predicted by Equation (19) is greater than that observed experimentally. The error is greatest for 3/8-in. tubes at low gas velocities and 7/8-in. tubes at high gas velocities. Single, round tubes were studied by Govier et al. (*13, 14*). Those of the present work were square and arranged in parallel sections. These factors may have caused the deviation of the predicted results.

A correction could be applied to the literature values for the friction factor and the resulting modified friction factor was capable of representing the results for the present system. A liquid leg was attached to the column at the level of the tray. During operation this leg indicated the sum of the liquid head and the frictional loss. The clear liquid height was determined by an independent method and was subtracted from the reading of the liquid leg. The two-phase friction factor necessary to account for this frictional loss was then computed. It was determined that the relationship between the literature values of the friction factor to those of the present study was

$$f'_{LM} = (53.3\,D - 2.96)\,(f'_L - 0.007) + 0.014 \quad (21)$$

The total pressure drop was the sum of the three components:

$$h_{\text{total}} = h_{\text{orifice}} + h_{\text{liquid head}} + h_{\text{friction}} \quad (22)$$

The range of error in estimating the total pressure drop by Equation (22) with the use of the unmodified friction factor in Equation (19) was − 20 + 25%. The modified friction factor reduces this range to ± 12%, with an average error of − 1%.

The pressure drop observed in the supported froth equipment is comparable to that of cross-flow sieve trays or bubble cap trays. At equivalent total mass flow rates [lb./(hr.) (sq. ft.)] of the gas and liquid phases Mayfield et al. (*21*) observed about 1.5 to 3.5 in. of water. Warzel and Williams (35) observed about 2 to 4 in. of water for a bubble cap tray. The pressure drop of the supported froth equipment was about 2 to 3 in. of water for comparable mass flow rates.

Liquid and Gas Velocity

Three packing sizes were studied: 3/8-, 5/8-, and 7/8-in. The liquid rate was 1,000 lb./(hr.) (sq. ft.) Spacing was maintained at 1/2 in. The results are shown in Figure 7, a plot of upward liquid velocity vs. gas rate with packing size as a parameter. The liquid velocity is relative to the wall.

The gas velocity was computed from the known values of gas flow rate, column dimensions, and liquid holdup. The superficial gas velocity based on the total cross sectional area of the column was

$$Ug = \frac{\text{area}}{\text{volumetric flow rate}} \quad (23)$$

The velocity of the bubbles depends upon the froth density and can be computed from

$$U'_B = \frac{Ug}{1 - h_1/h_2} \quad (24)$$

U'_B is relative to the wall.

Liquid-to-Gas Ratio

It is important in mass transfer calculations to know the ratio of the amount of liquid to gas which contact each other in the vertical tubes. The amount of gas was determined from the known volumetric flow rate. The amount of liquid was computed from the fraction of the total volume of the vertical tubes occupied by liquid (as determined by froth density) and the upward velocity of liquid determined from Figure 7.

Bubble Size

Bubble size data were obtained from photographs as explained earlier. The mean bubble diameter was taken as the average value. When large bubbles were encountered it became necessary to consider the shape of the bubble when the 3/8-in. packing was run. The larger

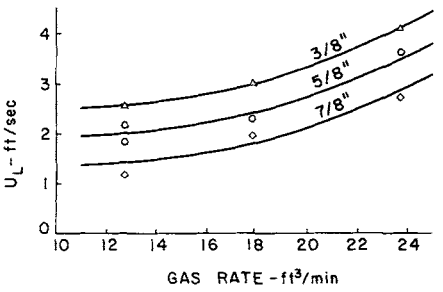

Fig. 7. Upward liquid velocity vs. gas rate; packing size as parameter.

TABLE 2. AVERAGE BUBBLE SIZE AND CONTACT TIME FOR THE AMMONIA-AIR-WATER SYSTEM

L, lb./(hr.) (sq. ft.)	G, lb./(hr.) (sq. ft.)	a, cm.	t_g, sec.	L, lb./(hr.) (sq. ft.)	G, lb./(hr.) (sq. ft.)	a, cm.	t_g, sec.
Packing*—1-4, ⅜ (½)				Packing*—2-4, ⅜ (½)			
800	515	0.43	0.142	1,000	515	0.38	0.143
	720	0.41	0.112		720	0.37	0.118
	955	0.38	0.094		955	0.37	0.101
1,000	515	0.40	0.148				
	720	0.40	0.118				
	955	0.38	0.095				
Packing*—1-4, ⅝ (½)				Packing*—None			
500	515	0.43	0.184	1,000	515	0.74	0.107
750	515	0.40	0.156		720	0.60	0.071
	720	0.41	0.166		955	0.46	0.053
1,000	515	0.37	0.155				
	720	0.38	0.128				
	955	0.37	0.101				

* See first footnote in Table 1.

bubbles were somewhat deformed into a cylindrical shape by the packing. For the elongated bubbles the average diameter was taken as the diameter of an equivalent sphere which would show the same unsteady state diffusional efficiency as the actual configuration. A cross plot of the solutions for the approach to equilibrium for the sphere, cylinder, and plane given by Crank (*6*) can be constructed which has aspect ratios of the cylinder as a parameter.

The bubble size was found to be smaller for the ammonia-air-water system, due perhaps to the lower surface tension of this system.

Comparison of Predicted and Observed Mass Transfer Efficiencies

The application of the proposed model will now be demonstrated in predicting the efficiency of the supported froth equipment.

k_L was predicted from Equation (2) by the substitution of necessary parameters. Diffusion coefficients were taken from Reid and Sherwood (*26*). Bubble velocities relative to the liquid were determined as the difference between the velocity of the liquid taken from Figure 7 and the gas velocity relative to the wall. Bubble sizes were taken from Table 2 or 3.

The parameter Γ was computed from this value of k_L, along with values of a from Tables 2 and 3, diffusivity from Reid and Sherwood (*26*), and Henry's constant (*5*). For the spherical bubbles the surface renewal time was taken as the time required for the bubble to move through its diameter relative to the liquid. For the elongated bubbles the surface renewal time was taken as the time for the bubble to move through its length. In general Γ was on the order of 0.01 for carbon dioxide and 1,000 for ammonia.

As anticipated from previous work the ammonia-air-water system gave indications of having a dependence upon the liquid phase under certain conditions. When packing was used the agitation of the liquid phase was pronounced and the system appeared to be near true gas phase controlled. For runs made without packing the agitation was less and the resistance of the liquid phase again became important. A correction for no packing was made by adjusting the predicted value of Γ. Pertinent data have been summarized by Sherwood and Pigford (*29*). These data show that k_g values obtained for true gas-controlled transfer such as humidification are from two to three times greater than values of k_{og} obtained from ammonia absorption experiments under similar conditions. In the present work the ratio of k_g/k_{og} was taken as 2.5. For ammonia runs made without packing the

TABLE 3. AVERAGE BUBBLE SIZE AND CONTACT TIME FOR CARBON DIOXIDE-AIR-WATER SYSTEM

L, lb./(hr.) (sq. ft.)	G, lb./(hr.) (sq. ft.)	a, cm.	t_g, sec.	t_r, sec.	t_r', sec.	L, lb./(hr.) (sq. ft.)	G, lb./(hr.) (sq. ft.)	a, cm.	t_g, sec.	t_r, sec.	t_r', sec.
Packing*—1-4, ⅜ (½)						Packing*—1-4, ⅞ (½)					
1,000	515	0.59	0.132	0.042	0.090	1,000	515	0.75	0.107	0.0045	0.032
	720	0.57	0.14	0.027	0.036		720	0.70	0.108	0.035	0.037
	955	0.53	0.085	0.028	0.052		955	0.68	0.098	0.028	0.039
750	515	0.58	0.120	0.042	0.090						
	720	0.58	0.096	0.027	0.036						
	955	0.54	0.077	0.028	0.052						
Packing*—2-4, ⅜ (½)						Packing*—None					
1,000	720	0.57	0.108	0.042		1,000	515	0.65	0.115	0.020	
							720	0.65	0.073	0.015	
Packing*—1-4, ⅝ (½)							955	0.63	0.049	0.012	
						750	515	0.65	0.103	0.020	
1,000	515	0.73	0.138	0.029	0.052		720	0.63	0.0706	0.015	
	720	0.69	0.110	0.025	0.051	500	515	0.66	0.103	0.020	
	955	0.65	0.085	0.016	0.061		720	0.66	0.068	0.015	
750	720	0.70	0.106	0.022	0.051		955	0.60	0.041	0.020	
500	720	0.70	0.099	0.022	0.051						
Packing*—2-4, ⅝ (½)											
1,000	515	0.73	0.142	0.029	0.052						
	720	0.69	0.118	0.022	0.051						
	955	0.66	0.095	0.016	0.061						

* See first footnote in Table 1.

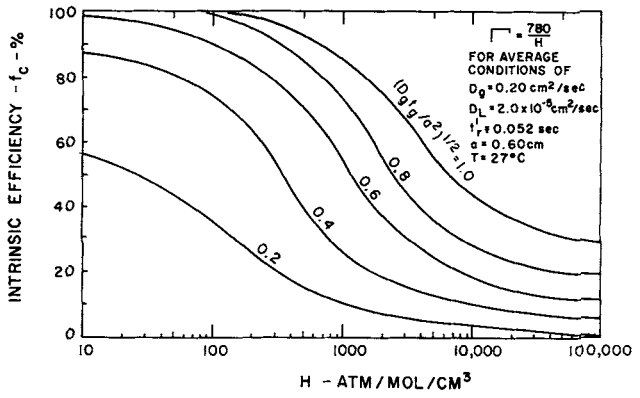

Fig. 8. Intrinsic efficiency (f_c) vs. solubility constant (H) with $(D_g t_g/a^2)^{1/2}$ as parameter.

predicted value of the group a/D_g in Γ was decreased by this factor.

For the computation of $(D_g t_g/a^2)^{1/2}$, total contact time for a bubble was taken as time for the bubble to move the height of the froth, that is, the froth height divided by the bubble velocity. D was again taken from Reid and Sherwood (*26*) and a from Tables 2 and 3.

The values of L/G for the cocurrent flow of liquid and gas were computed from liquid velocity from Figure 7, and froth density (h_l/h_2) computed from the previous correlations; m was computed from these L/G values. Values of f_s were read from Figure 1. Finally, these were converted to values of f_c by Equation (12).

For all runs with froth supporting packing and the ammonia-air-water system, the maximum deviation of the predicted value from the average value was +7.2% to −16%; the average was +3.7% to −3.6%. A complete sample calculation, tabulation of results of the calculation procedure, and the deviation of the predictions from the observed values can be found in reference 39.

The efficiency of the supported froth system varied from about 80 to 95%; without packing the efficiency was about 30 to 50%. This is generally better than that obtained by Gerster, Hill, Hochgraf, and Robinson (*12*) for conventional sieve trays and bubble cap trays. On a comparable basis, the range of efficiency in reference *12* was about 70 to 90%.

The efficiency for the carbon dioxide-air-water system varied from about 1 to 5%. Although this system shows a low efficiency, it is comparable to other equipment. Tarat et al. (*31a*) found efficiencies of from 1 to 10% for contact times of from 0.115 to 0.27 sec. The equipment was a single tray froth apparatus.

The agreement between predicted and observed results are not as good for the carbon dioxide-air-water system as for the ammonia-air-water system. Although the predicted curves show the correct trends and are correctly oriented with respect to each other, they are consistently high. The deviation of the predicted value averaged only 1.5% above the predicted value, but because the efficiency was quite low this gave an average error of +54%. Experimental error could have contributed to this discrepancy. It is felt, however, that a more serious error was made in the assumptions concerning the nature of the fluid behavior near the gas-liquid interface. It was assumed that the surface renewal time was the time required for the bubble to move one diameter relative to the liquid. This is a critical assumption for liquid phase controlled systems. Hydrodynamic factors such as the wake of a preceding bubble may be expected to affect the liquid flow patterns.

The model may be used to predict a closer estimate of the efficiency by replacing the surface renewal time computed at $2a/U_B$ by an effective surface renewal time. If it is assumed the deviation of the predicted efficiency is caused by an error in estimating t_r to be $2a/U_B$, t_r can be corrected by reverse calculation, with the experimental efficiency data to give an effective surface renewal time t'_r. Effective surface renewal times have been computed and are shown in Table 3.

All data can be represented by a general correlation if average values are assigned to certain variables. If values of fluid properties are computed for an average temperature of 27°C., then for ammonia, $D_g = 0.22$ and $D_l = 2.0 \times 10^{-3}$ sq. cm./sec. For carbon dioxide $D_g = 0.16$ and $D_L = 2.1 \times 10^{-5}$ sq.cm./sec. These quantities show only small variations over a moderate range of temperature. Table 3 shows an average t'_r of 0.052 sec. An average bubble size of 0.60 cm. will be assumed.

The major factor which influences Γ is the solubility (given by H). This may be seen by rearranging Equation (8) to

$$\Gamma = \frac{RT}{D_g H}\sqrt{\frac{2D_L}{\pi}}\sqrt{aU_B}$$

Under the assumptions of the present model, the quantities in the first group will be relatively unaffected by gas and liquid rates. The particular system under consideration will have a major effect on the value of the group because of the variation in H. For instance, $H = 30,600$ for carbon dioxide, and 20.2 for ammonia. Two factors enter into the consideration of the group $\sqrt{aU_B}$. First, it will vary only as the square root of the product and second, it is noted that changes in gas rate change these quantities in opposite directions, thereby compensating for changing bubble size and bubble velocity. From these considerations an average value of Γ may be determined which will be primarily affected by change in H.

A similar argument as given above can be applied to the determination of the exponent m in Equation (12). Comparison shows that the value of H is the most significant factor in determining the value of m.

With these assumptions the average value of Γ is

$$\Gamma = \frac{780}{H}$$

The average value of m is about 5.4. With these assumptions a general plot of f_c vs. H with $(D_g t_g/a^2)^{1/2}$ as a parameter may be constructed. Figure 8 is the resulting plot.

The value of the group $(D_g t_g/a^2)^{1/2}$ will be affected by gas and liquid rates and packing size as these affect froth height and froth density (thereby influencing the contact time) and the bubble size.

CONCLUSIONS AND RECOMMENDATIONS

A mass transfer device utilizing supported high density froth has been described. The range of gas rates for which the column will operate is considerably greater than for conventional sieve trays or for the present dual-flow tray operated without packing. The range of liquid rates is somewhat less than for conventional sieve trays.

The pressure drop can be considered to be the sum of an orifice effect, clear head of liquid, and two-phase frictional loss. The pressure drop can be predicted from existing analytical expressions if a modified friction factor is applied to the two-phase frictional loss. In general, the pressure drop is comparable to other equipment.

The efficiency of the supported froth equipment is better than comparable conventional sieve and bubble cap trays for gas phase controlled systems. It is comparable for liquid phase controlled systems. The efficiency is definitely improved by the use of packing.

A model which uses measurable physical parameters has been developed. A general correlation based on the model has been developed.

This study has shown that the supported froth equipment is capable of producing high efficiency and a wide range of operation. The chief disadvantage of the supported froth equipment was the lower liquid phase efficiency, caused primarily by the low solubility of the carbon dioxide. (see Figure 8). However, this effect can be influenced for most systems of low solubility by the use of a reactive solution.

The need for further work in at least two areas is indicated. Additional work should be done with different packings—perhaps more sections of shorter height. More work should be done on the design of the sieve plate itself with the purpose of modifying the gas and liquid rates which could be run. Design information for the dual-flow tray is limited.

ACKNOWLEDGMENT

The authors wish to thank the U.S. Public Health Service for its financial assistance.

NOTATION

a = average bubble radius, cm.
$a_{1\ldots5}$ = constant
B = constant, Equations (5) and (6)
C = liquid concentration, mole/cc.
D = diffusivity, cc./sec.
D' = diameter of vertical tubes, ft.
f_c = intrinsic efficiency or fractional instantaneous approach to equilibrium for cocurrent flow
f_s = intrinsic efficiency for perfectly mixed liquid phase
f'_L = two-phase friction factor, Equation (24)
f'_{LM} = modified two-phase friction factor, Equation (25)
$\Delta F/\Delta X$ = pressure drop per foot of height, Equations (23) and (24), ft. of fluid/ft.
G = gas flow rate, lb./(hr.) (sq. ft.)
G' = gas flow rate, cu. ft./min.
G'' = gas flow rate in orifice equation, cu.ft./(min.) (hole)
H = Henry's law constant, atm./(mole) (sq. cm.)
h = pressure drop, in. of water
h_1 = clear liquid height on tray, in.
h_2 = froth height, in.
k_g = gas phase mass transfer coefficient, moles/(sq. cm.) (sec.) (mole)/cc.
k_L = liquid phase mass transfer coefficient, moles/(sq. cm.) (sec.) (mole)/cc.
L = liquid flow rate, lb./(hr.) (sq. ft.)
L' = liquid flow rate, cu. ft./min.
MW = molecular weight
m = exponent
P = pressure, atm. or lb./sq. in.
Q = exponent, see Table 1.
R = gas law constant, 82.06
R_v = ratio of gas to liquid volume in vertical tubes, cu. ft./cu. ft.
S = packing spacing, in.
T = temperature, °K. or °R.
t_g = total contact time for a bubble, sec.
t_r = surface renewal time for a bubble, sec.
t'_r = effective surface renewal time for a bubble, sec.
U_g = superficial gas velocity Equation (23), ft./sec. or cm./sec.
U'_b = bubble velocity relative to wall, cm./sec.
U_b = bubble velocity relative to liquid, cm./sec.
U_l = liquid velocity relative to wall, cm./sec. or ft./sec.
W = exponent, see Table 1
Z = compressibility factor

Greek Letters

α = constant of proportionality
Δ = change
e = logarithm base, 2.718
Γ = parameter, see Equations (5), (6), and (7)
ρ_f = froth density, h_1/h_2

Subscripts

1 = top of column
2 = bottom of column
G or g = gas
L or l = liquid
i = initial
f = final
n = integer

LITERATURE CITED

1. Arnold, D. S., C. A. Plank, and E. M. Schonborn, *Chem. Eng. Progr.*, **48**, 633 (1952).
2. *Brit. Chem. Eng.*, **2**, 544 (1957).
3. Calvert, Seymour and Walter Workman, *Talanta*, **4**, 89 (1960).
4. ————, *Am. Ind. Hygiene Assoc. J.*, **22**, 318 (1961).
5. "Handbook of Chemistry and Physics," 43 ed., Chemical Rubber Publishing Co., Cleveland, Ohio (1961).
6. Crank, J., "Mathematics of Diffusion," Oxford Univ. Press, London (1956).
7. Foss, A. S., J. A. Gerster, and R. L. Pigford, *A.I.Ch.E. J.*, **4**, 231 (1958).
8. Gasiuk, G. N., A. G. Bolshakov, A. V. Kortnev, and P. la. Krainiti, *J. Appl. Chem. U.S.S.R.*, **31**, 1013 (1958).
9. Geddes, R. L., *Trans. Am. Inst. Chem. Engrs.*, **42**, 79 (1946).
10. Gerster, J. A., A. P. Colburn, W. E. Bonnet, and T. W. Carmody, *Chem. Eng. Progr.*, **45**, 717 (1949).
11. Gerster, J. A., W. E. Bonnet, and I. Hess, *ibid.*, **47**, 523 (1951).
12. Gerster, J. A., A. B. Hill, N. N. Hockgraf, and D. G. Robinson, "Tray Efficiencies in Distillation Column," Final Rept., Univ. Delaware, New York (1958).
13. Govier, G. W., B. A. Radford, and J. S. C. Dunn, *Can. J. Chem. Eng.*, **35**, 58 (1957).
14. Govier, G. W., and W. L. Short, *ibid.*, **36**, 195 (1958).
15. Higbie, R., *Trans. Am. Inst. Chem. Engrs.*, **31**, 365 (1935).
16. Huang, C.-J., and J. R. Hodson, *Petrol. Refiner*, **37**, 103 (February 1958).
17. Hughmark, G. A., and H. E. O'Connell, *Chem. Eng. Progr.*, **53**, 3, 127 (1957).
18. Hunt, C. d'A., D. N. Hanson, and C. R. Wilkie, *A.I.Ch.E. J.*, **1**, 441 (1955).
19. Kolthoff, I. M., and E. B. Sandell, "Textbook of Quantitative Inorganic Analysis," Macmillan, New York (1952).
20. Lobo, W. E., L. Friend, F. Hashmall, and F. Zenz, *Trans. Am. Inst. Chem. Engrs.*, **41**, 693 (1945).
21. Mayfield, F. D., W. L. Church, Jr., A. C. Green, D. C. Lee, Jr., and R. W. Rasmussen, *Ind. Eng. Chem.*, **44**, 2238 (1952).
22. McAllister, R. A., P. H. McGinnis, Jr., and C. A. Plank, *Chem. Eng. Sci.*, **9**, 25 (1958).
23. MURA (Multiple Regression Analysis), Case Inst. Technol. Tech. Rept. 1054, Cleveland, Ohio (1961).
24. O'Connell, H. E., *Trans. Am. Inst. Chem. Engrs.*, **42**, 741 (1946).
25. Perry, J. H., "Chemical Engineers Handbook," 3 ed., McGraw-Hill, New York (1950).
26. Reid, R. C., and T. K. Sherwood, "The Properties of Gases and Liquids," McGraw-Hill, New York (1958).
27. Rodinov, A. I., and V. F. Marchenkov, *J. Appl. Chem. U.S.S.R.*, **33**, 1094 (1960).
28. *Ibid.*, 2005.
29. Sherwood, T. K., and R. L. Pigford, "Absorption and Extraction," McGraw-Hill, New York (1952).

30. Sherwood, T. K., G. H. Shipley, and F. A. L. Holloway, *Ind. Eng. Chem.*, **30**, 765 (1938).
31. Stone, H. C., Sc.D. thesis, Massachusetts Inst. Technol., Cambridge (1953).
31*a*. Tarat, E. Ya., and S. A. Bogatykh, *J. Appl. Chem. U.S.S.R.*, **34**, 1846 (1961).
32. Gasyuk, G. N., A. G. Bol'shakov, A. V. Kortnev, and P. Ya. Krainil, *ibid.*, **32**, 792 (1959).
33. Yarlamov, M. L., G. A. Manakin, and Ya. I. Starosel'skii, *ibid.*, 2504.
34. Walter, J. F., and T. K. Sherwood, *Ind. Eng. Chem.*, **33**, 493 (1941).
35. Warzel, L. A., and B. Williams, "Absorption Studies Tray Efficiency Research Program," Am. Inst. Chem. Engrs., New York (1955).
36. West, F. B., W. B. Gilbert, and T. Shimizu, *Ind. Eng. Chem.*, **44**, 2470 (1952).
37. Wilkie, E., *Z. Anorgan. Allegem. Chem.*, **119**, 365 (1921).
38. Workman, W. L., and Seymour Calvert, paper presented at Am. Ind. Hygiene Assoc. Conf. (May, 1962).
39. Workman, W. L., Ph.D. thesis, Case Inst. Technol., Cleveland, Ohio (1963).

Manuscript received February 1, 1963, revision received February 7, 1966; paper accepted February 8, 1966. Paper presented at A.I.Ch.E. New Orleans meeting.

Optimality and Computational Feasibility in Transient Control: Part I. A Modified Criterion for Optimality

W. O. PARADIS
University of Illinois, Urbana, Illinois

D. D. PERLMUTTER
University of Pennsylvania, Philadelphia, Pennsylvania

The notion of optimality with regard to transient control is critically examined with a particular view toward the computational difficulties of solving the optimal control problem, and the arbitrary aspects of the usual objective functions. Realizing a need for effective approximations, a criterion for transient control is developed which requires a minimum of computational effort to apply in practice. Optimality is achieved in an instantaneous sense, and it is argued that overall optimality is well approximated for many cases of practical interest. To demonstrate its use, the criterion is applied to the transient control of a stirred-tank reactor. Numerical examples are given and the results are discussed and compared with those obtained by alternative methods.

The subject of mathematical optimization is intimately tied to the matter of objectives. The very concept of optimality is, in fact, predicated upon the notion that the numerous factors which determine the quality of performance can be combined and properly accounted for by a single performance index. Perhaps maximum net profit is the most meaningful of many possible indicators of optimality, but the formulation of such an index of performance requires a detailed economic analysis involving many factors, some (such as safety) difficult to judge accurately in terms of monetary values. Although performance indices have been devised in this manner (5), the arbitrary quality of the performance index is difficult to eliminate altogether. As more factors are taken into consideration, the objective function becomes unwieldy and of limited usefulness in obtaining practical solutions to the control problem.

Optimization with respect to other indices of performance may be viewed as an expedient means of approximating the condition of maximum profit. For example, it is sometimes required that the system attain a desired state in the minimum possible time (*11, 13*). Although such a strategy is generally compatible with a desire for maximum profits, it is not difficult to conceive of instances where a higher return would result from an increase in the duration of the transient: perhaps the cost of time optimal control is excessive or the product quality is poor. Similarly, minimizing some other performance index, say, mean square deviation of a critical state variable, might more or less approximate maximum profit. It is thus important to bear in mind in comparing various strategies of control that each is based on a somewhat arbitrary measure of effectiveness. Although superficially the object of control may be to minimize rigorously some particular performance index, the index itself must be subjectively formulated. Whether the resulting control is acceptable or not must be determined by the designer. From an engineering point of view the decision on a suitable objective function does not entirely precede the optimization but is, in an important sense, part of it.

These considerations not withstanding some measure of system performance must be chosen. One common form of the optimal control problem is to determine that control policy $\mathbf{u}(t)$ which minimizes the reasonable but of necessity somewhat arbitrary criterion: